Title
PTEN deletion enhances the regenerative ability of adult corticospinal neurons

Journal
Nature Neuroscience, 13(9)

ISSN
1097-6256

Authors
Liu, Kai
Lu, Yi
Lee, Jae K
et al.

Publication Date
2010-09-01

DOI
10.1038/nn.2603

HHS Public Access

Author manuscript

Nat Neurosci. Author manuscript; available in PMC 2011 March 01.

Published in final edited form as:

Nat Neurosci. 2010 September ; 13(9): 1075–1081. doi:10.1038/nn.2603.

PTEN Deletion Enhances the Regenerative Ability of Adult Corticospinal Neurons

Kai Liu[1,*], **Yi Lu**[1,*], **Jae K. Lee**[2], **Ramsey Samara**[2], **Rafer Willenberg**[3], **Ilse Sears-Kraxberger**[3], **Andrea Tedeschi**[1], **Kevin Kyungsuk Park**[1], **Duo Jin**[1], **Bin Cai**[1], **Bengang Xu**[1], **Lauren Connolly**[1], **Oswald Steward**[3], **Binhai Zheng**[2], and **Zhigang He**[1,#]

[1] F.M. Kirby Neurobiology Center, Children's Hospital, and Department of Neurology, Harvard Medical School, 300 Longwood Avenue, Boston, MA 02115, USA

[2] Department of Neurosciences, University of California San Diego, 9500 Gilman Drive, La Jolla, California, 92093, USA

[3] Reeve-Irvine Research Center, University of California at Irvine College of Medicine; Department of Anatomy & Neurobiology, Neurobiology & Behavior and Neurosurgery, Irvine, California, 92697, USA

Abstract

Despite the essential role of the corticospinal tract (CST) in controlling voluntary movements, successful regeneration of large numbers of injured CST axons beyond a spinal cord lesion has never been achieved. Here we demonstrate a critical involvement of PTEN/mTOR in controlling the regenerative capacity of mouse corticospinal neurons. Upon the completion of development, the regrowth potential of CST axons lost and this is accompanied by a down-regulation of mTOR activity in corticospinal neurons. Axonal injury further diminishes neuronal mTOR activity in these neurons. Forced up-regulation of mTOR activity in corticospinal neurons by conditional deletion of *PTEN*, a negative regulator of mTOR, enhances compensatory sprouting of uninjured CST axons and even more strikingly, enables successful regeneration of a cohort of injured CST axons past a spinal cord lesion. Furthermore, these regenerating CST axons possess the ability to reform synapses in spinal segments distal to the injury. Thus, modulating neuronal intrinsic PTEN/mTOR activity represents a potential therapeutic strategy for promoting axon regeneration and functional repair after adult spinal cord injury.

Spinal cord injury often results in permanent paralysis, largely due to the failure of injured axons to regenerate in the adult mammalian central nervous system (CNS). In principle, functional recovery after CNS injury could be achieved by two forms of axonal regrowth:

#To whom correspondence should be addressed. zhigang.he@childrens.harvard.edu.
*These authors contribute equally.

Supplementary information is included with this manuscript.

AUTHOR CONTRIBUTIONS

KL, YL, JKL, RS, RW, ISK, AT, KKP, DJ, BC, BX, LC, OS performed experiments and analyses. KL, JKL, OS, BZ and ZH drafted and edited the paper.

sprouting of spared non-injured axons to form new circuits compensating for the lost functions, and regeneration of lesioned axons that can potentially re-form the lost connections[1,2]. Among different types of long-projecting descending tracts, the CST that controls voluntary movements is particularly important for functional recovery after spinal cord injury[3,4]. Despite numerous previous efforts to stimulate both collateral and regenerative growth of CST axons in experimental injury models[1–4], success has been very limited[5–7], suggesting that injured CST axons are especially refractory to regeneration. For instance, removing extracellular inhibitory molecules allows some sprouting of spared CST axons but very limited regeneration of injured axons[8–10]. Delivery of neurotrophic factors promotes some degree of regeneration in certain types of axons such as optic nerve axons from retinal ganglion neurons[11], but fails to elicit regeneration of injured CST axons after spinal cord injury[12,13]. While over-expressing the BDNF receptor TrkB can promote CST axon regrowth into a BDNF-expressing graft after a subcortical injury[14], it is unknown whether this finding can be extended to spinal cord injury. Furthermore, although grafting permissive substrates at the spinal cord injury site permits some sensory axons and brainstem-derived axons to grow into the graft, CST axons show minimal growth[15,16]. Even at early postnatal stages, most injured CST axons fail to grow into a permissive graft, although axons of other neural systems are capable[17]. These findings have instilled doubt as to whether it is even possible to develop a strategy to stimulate regeneration of large numbers of injured CST axons after spinal cord injury.

We recently discovered that the age- and injury-dependent down-regulation of neuronal mTOR activity is a major cause of the lack of regeneration of optic nerve axons after injury, and that genetic activation of mTOR promotes successful optic axon regeneration[18]. However, it is unknown whether this is specific to retinal ganglion neurons or applicable to other CNS neurons. Here, we show that enhancement of the mTOR pathway strikingly enhances regrowth (both sprouting and regeneration) of adult CST axons following different types of injury models.

RESULTS

Correlation between mTOR down-regulation and repression of CST sprouting

We first investigated whether mTOR activity regulates the sprouting responses of CST axons after unilateral pyramidotomy[19,20] (Supplementary Fig. 1). In this model, the CST was severed unilaterally at the left medullary pyramid above the pyramidal decussation. The anterograde tracer biotinylated dextran amine (BDA) was injected to the right sensorimotor cortex to label uninjured CST axons. In intact mice, most labeled axons were detected on the left side of the spinal cord, with few axons appearing in the right side (Fig. 1a,c). Thus increased numbers of labeled axons in the right side of the spinal cord following a pyramidotomy would represent trans-midline sprouting of intact CST axons into the denervated side.

By this procedure, we found a sharp age-dependent decline in trans-midline sprouting responses: while left pyramidotomy at postnatal day 7 (P7) induced massive trans-midline sprouting of CST axons from the uninjured side (Fig. 1b,e,g), the same injury in 2-month old mice led to minimal CST sprouting (Fig. 1d,e,g). To assess mTOR activity in cortical

neurons of different ages, we performed immunohistochemistry on cortical sections using anti-phospho-S6 (p-S6) antibodies, an established marker of mTOR activation[18]. Immunostaining for p-S6 is dramatically reduced in most of adult cortical neurons (Fig. 1i) compared with that in P7 brains (Fig. 1h), suggesting a correlation between the down-regulation of the mTOR activity and the decrease in the compensatory sprouting ability of cortical neurons.

PTEN deletion prevents mTOR down-regulation and increases CST sprouting

We next examined whether preventing the age-dependent mTOR down-regulation could enhance the sprouting responses of adult CST axons. Our strategy was to use Cre-expressing adeno-associated virus (AAV-Cre) to delete the gene encoding PTEN, a negative regulator of mTOR[21], in homozygous conditional PTEN mutant (*PTEN*$^{f/f}$) mice[22]. As a validation of the strategy, we found that injection of AAV-Cre, but not AAV-GFP virus, into the sensorimotor cortex of a Cre-reporter mouse (Rosa26-lox-STOP-lox-PLAP[23]), induced efficient Cre-dependent PLAP expression in neurons throughout the sensorimotor cortex (Supplementary Fig. 2).

To assess whether *PTEN* deletion elevates neuronal mTOR activity, we injected AAV-Cre into the sensorimotor cortex of *PTEN*$^{f/f}$ mice at P1 and examined the p-S6 signal in the adult. Indeed, compared to AAV-GFP injected *PTEN*$^{f/f}$ controls (Fig. 1k, 2b–d, 2n), immunostaining for p-S6 was significantly higher in adult *PTEN*-deleted cortical neurons (Fig. 1j, 2h–j, 2n). This postnatal AAV-Cre-mediated *PTEN* deletion does not appear to alter the projections of CST axons in the spinal cord, as the numbers and termination patterns of labeled axons in the pyramids and different levels of spinal cord are not significantly different in the *PTEN*$^{f/f}$ mice injected with either AAV-Cre or AAV-GFP (Supplementary Fig. 3). This result is consistent with the observation that the development of CST projections is largely complete in the early postnatal stage[24].

We next performed pyramidotomy in adult *PTEN*$^{f/f}$ mice which had a neonatal injection of AAV-Cre or AAV-GFP. Compared to the limited sprouting in controls (Fig. 3a–l,q,r), *PTEN* deletion elicited extensive trans-midline sprouting of adult CST axons from the intact side into the denervated side (Fig. 3m–r). Thus, *PTEN* deletion is sufficient for maintaining high mTOR activity characteristic of young neurons in adult cortical neurons, and for these neurons to launch a robust sprouting response after injury.

CST regeneration after T8 dorsal hemisection after neonatal *PTEN* deletion

Although sprouting of uninjured neurons might partially compensate for lost function, inducing severed axons to regenerate beyond the lesion site and to re-connect the axonal pathways would be needed for functional recovery in more severe injuries. We thus asked whether *PTEN* deletion would sustain a high level of mTOR activity in injured adult corticospinal neurons and elicit robust axon regeneration. By immunohistochemistry we found that axotomy diminished p-S6 levels in adult corticospinal neurons identified by retrograde labelling (Fig. 2e–g,n). With the stepwise down-regulation of mTOR activity, firstly an age-dependent decline (Fig. 1h,i) and secondly an injury-triggered further reduction (Fig. 2b–g,n), lesioned adult corticospinal neurons exhibited low p-S6 signal,

suggesting a major reduction of mTOR activity. Importantly, AAV-Cre-mediated *PTEN* deletion not only increased basal p-S6 levels (Fig. 2h–j,n) but also efficiently attenuated the injury-induced loss of mTOR activity in corticospinal neurons (Fig. 2k–n).

Having established an experimental paradigm to maintain a relatively high level of mTOR activity in adult corticospinal neurons even after injury, we set out to determine whether *PTEN* deletion would enable regenerative growth of adult CST axons in two different spinal cord injury paradigms (supplementary Fig. 4): a dorsal hemisection, which transects all traced CST axons but spares the ventral spinal cord[25–28], and a complete crush model that transects all passing axons and leaves no bridge of uninjured tissue[29,30].

Dorsal hemisection injuries were created at T8 (Supplementary Fig. 4b), and the CST from one hemisphere was traced 6 weeks post-injury by injecting BDA into the right sensorimotor cortex, allowing the mice to survive for two additional weeks. Transverse sections 5 mm caudal to the lesion sites were first examined. The presence of any labeled axons in the dorsal main tract and the dorsolateral tract caudal to the injury was taken as evidence of incomplete lesions and these animals were excluded from further analysis.

In 9 control mice, not a single CST axon was seen extending directly through the lesion site (Fig. 4a–b). In two of these control mice, we found a few axons extending to the distal spinal cord via the ventral column, consistent with previous observations[28]. Instead, characteristic dieback of CST axons from the injury site was observed (Fig. 4a–b, Supplementary Fig. 5a), and individual axons displayed numerous retraction bulbs (Supplementary Fig. 5c,e). By contrast, when PTEN was deleted, the main CST bundle extended to the very edge of the lesion margin (Fig. 4c–d, Supplementary Fig. 5b) and few retraction bulbs were associated with the labeled CST axons eight weeks after injury (Supplementary Fig. 5d,e). This phenotype could be due to either a lack of axon dieback of *PTEN*-deleted neurons, or resumed axon regrowth after the initial injury-induced retraction. To distinguish between these, we examined CST axons at 10 days post-injury. Apparent dieback and large numbers of retraction bulbs were observed at this early time point in both control and *PTEN*-deleted axons (Supplementary Fig. 6). Thus, instead of affecting the acute post-injury axonal degeneration, *PTEN*-deletion likely reversed the normal abortive regenerative attempts typical for injured adult CNS axons[31] and enhanced their regrowth.

More strikingly, significant numbers of labeled axons regenerated past the lesion site in all 11 *PTEN*-deleted mice (Fig. 4c–g). Examination of the entire collection of serial sections from these animals (one example shown in Supplementary Fig. 7) revealed two distinct routes by which labeled CST axons reached the caudal spinal cord: either directly growing through the lesion (arrows in Fig. 4e) or circumventing the injury site via the spared ventral white matter (arrowheads in Fig. 4e). We estimated that approximately two thirds of labeled axons seen in the distal spinal cord grew through the lesion site and the rest projected along the ventral white matter. Critically, CST axons that regenerated past the lesion were not restricted to one side of the distal spinal cord and instead projected bilaterally (Supplementary Fig. 7, image #25 marks the midline). This is important because normal CST projections are largely unilateral. The presence of significant numbers of CST axons on

the side contralateral to the main tract is strong evidence of regenerative growth and cannot be accounted for by spared axons.

Importantly, similar results were obtained in an independent set of experiments where the lesions were performed in a double-blinded manner by an independent surgeon (Supplementary Fig. 8), who had carried out extensive analyses of possible CST regeneration in *Nogo* knockout mice[32]. In these experiments with control and *PTEN* deleted mice, the genotypes (AAV-Cre vs control) could be predicted by a blinded observer with great accuracy (~95%) based on BDA labeling (regenerator vs non-regenerator), further supporting the highly robust effect of *PTEN* deletion. Thus, the effect of *PTEN* deletion was consistent and robust enough to overcome the inter-investigator surgical variability typical for experimental spinal cord injury models.

Notably, the majority of *PTEN*-deleted regenerating axons projecting into the lesion site were associated with GFAP-positive tissue matrix (Fig. 4c,d, Supplementary Fig. 9c,d). These GFAP-positive matrixes often appeared in the superficial and medial locations of the spinal cord which would be highly unlikely, if not impossible, to be spared in a dorsal hemisection. GFAP-positive bridges were rarely seen at a shorter timeframe after injury (for example, Supplementary Figs. 6, 10 and 11), suggesting that these matrixes develop over time following dorsal hemisection, possibly as a consequence of an interaction between GFAP-negative cells and GFAP-positive cells at the injury site[33]. However, the identity of these GFAP-positive cells/or matrixes remains unknown.

CST regeneration after T8 complete crush injury after neonatal PTEN deletion

A complete spinal cord crush destroys all neural tissues at the injury site (Supplementary Fig. 4c) and is considered an extraordinary barrier for regeneration[29],[30]. In this model, the dura mater is not damaged so that the two ends of the spinal cord do not pull apart. In mice, the lesion site is filled with a connective tissue matrix[29],[30]. Initially, the matrix was largely GFAP negative, but evolved so that GFAP positive fingers extended into the connective tissue matrix at later post-injury stages (Supplementary Fig. 10).

At 12 weeks post-injury, no CST axons extended into or beyond the lesion site in any of the 8 control mice (Fig. 5a,b,e, Supplementary Fig. 12). In contrast, in all 8 $PTEN^{f/f}$ mice with AAV-Cre, numerous axons extended into the lesion sites and beyond the lesion for up to 3 mm (Figs. 5c–e, Supplementary Fig. 12). Many regenerating axons follow ectopic trajectories. For example, instead of projecting in one side of the spinal cord like normal CST axons, regenerating axons extended bilaterally with many of them showing tortuous projection patterns (Supplementary Fig. 12b,d, f), again, strongly against the possibility of being spared axons.

The results described above were obtained from the animals that had AAV-Cre injection at a neonatal age and spinal cord crush injury at 2 months of age. A question is whether such increased CST regeneration ability persists in corticospinal neurons in older mice. To assess this, we performed another set of experiments in which the same T8 spinal cord crush was performed in 5 month-old $PTEN^{f/f}$ mice with neonatal cortical injection of AAV-Cre or control. As shown in Supplementary Fig. 13, we found significant CST regeneration at 3

months post-injury in these mice, to an extent similar to what seen in the mice with injury at the age of 2 months (Fig. 5, Supplementary Fig. 12).

Deleting PTEN after the neonatal period can also induce CST regeneration

While no significant changes of CST numbers and projections were found in the spinal cord in *PTEN*$^{f/f}$ mice with neonatal AAV-Cre cortical injections (Supplementary Fig. 3), it is still possible that the up-regulation of mTOR activity associated with PTEN deletion at this early stage could block developmental events that turn off axon regeneration ability. To assess this, we first optimized a stereotaxic injection method to introduce AAVs to the sensorimotor cortex of mice at the age of 4 weeks. As shown in Fig. 6f, AAV-Cre injections resulted in efficient Cre-dependent PLAP expression in reporter mice. We estimated that in comparison to that with neonatal AAV-Cre injection (Supplementary Fig. 2), Cre-Dependent PLAP expression affected about 25% as much cortical area, likely due to less efficient diffusion of injected viral particles in the more mature cortex.

We then followed introduction of AAVs into the sensorimotor cortex of *PTEN*$^{f/f}$ mice at 4 weeks with a T8 complete spinal cord crush injury at the age of 8 weeks, and analyzed CST regeneration after 3 months post-injury. As shown in Fig. 6c–e, we still found significant CST regeneration in the spinal cord caudal to the lesion sites. Thus, *PTEN* deletion at both neonatal and young adult stages promoted robust CST axon regeneration past a complete spinal cord crush lesion.

Regenerating CST axons re-form synaptic structures

We next investigated whether regenerating CST axons from *PTEN*-deleted corticospinal neurons are able to form synapses. For this, we analyzed the samples taken from the gray matter of the spinal cord caudal to the lesion site in *PTEN*$^{f/f}$ mice with neonatal AAV-Cre injection and T8 crush injury at the age of 2 months. First, we assessed whether BDA-labeled regenerating CST axons are co-stained with vGlut1, a presynaptic marker for excitatory synapses[34–36]. As shown in Fig. 7a–i, some BDA-labeled bouton-like structures exhibit vGlut1-positive patches at the tip of BDA-labeled CST collaterals (Fig. 7b–d,f–h) and along the axonal length (Fig. 7f–h) and, suggesting the accumulation of the molecular machinery characteristic of a presynaptic terminal. We quantified these BDA and vGlut1-costained bouton-like structures in similar spinal cord locations in wild type intact mice and *PTEN*-deleted mice with crush injury. The incidence of vGlut1-positive patches in regenerating CST axons is approximately two thirds of that of CST axons in un-injured mice (Fig. 7i).

We further assessed whether BDA-labeled regenerated axons form synapses at the ultrastructural level. Sections from the spinal cords from *PTEN*-deleted mice with crush injuries and BDA injections were stained for BDA and further processed for electron microscopic analysis (Fig. 7j–l). We found many structures with characteristics of synapses, based on the presence of a contact zone with presynaptic vesicles (partially obscured by the reaction products in the labeled terminal) and a post-synaptic density (psd), as exemplified in Fig. 7j,k. For comparison, an unlabeled control synapse is shown in Fig. 7l. These results establish that regenerating CST axons from *PTEN*-deleted corticospinal neurons appear to

possess the ability to reform synapses in caudal segments. Whether these synapses are functional and the identity of the neurons contacted by the regenerated axons remain to be established.

DISCUSSION

Together, our results indicate that *PTEN* deletion enables injured adult corticospinal neurons to mount a robust regenerative response never seen before in the mammalian spinal cord. Both compensatory sprouting of intact CST axons and regenerative growth of injured CST axons are dramatically increased by *PTEN* deletion, suggesting that these two forms of regrowth share similar underlying mechanisms. PTEN inactivation is known to activates different downstream pathways such as Akt and mTOR signalling and inhibit other signalling molecules such as GSK-3[21,37,38] and PIP3[39]. In cortical neurons, mTOR activity undergoes a development-dependent down-regulation and axotomy further diminishes mTOR activity. On the other side, *PTEN* deletion in these neurons could increase mTOR activity and promote their regrowth ability. Together with our previous findings in retinal ganglion neurons[18], these results support a critical role of mTOR activity in determining the regrowth ability in CNS neurons. Because mTOR is a central regulator of cap-dependent protein translation[21], it is likely that neuronal growth competence is critically dependent on the capability of new protein synthesis, which provides building blocks for axonal regrowth. Other *PTEN* deletion-induced effects, such as increased axonal transport as the result of inactivation of GSK-3, might also be involved.

Our results also indicate that regenerating CST axons from *PTEN*-deleted corticospinal neurons are able to reform synapses in the spinal cord caudal to the lesion site. As CST axons that regenerate after *PTEN* deletion extend bilaterally in contrast to normal CST axons that extend unilaterally, it is unknown to what extents these regenerating axons could make synaptic connections with their original targets. Interestingly, at least in some species such as the larval lamprey[40] and goldfish[41], axons that regenerate past a spinal cord lesion fail to reach their original targets, yet make synapses that allow functional recovery. Thus, our future studies will be aimed to determine whether these regenerating axons and synapses could mediate functional recovery after spinal cord injury.

Notably, despite robust regenerative growth of CST axons rostral to a spinal cord injury in *PTEN* deleted mice, many robustly growing axons fail to penetrate into the GFAP-negative area at the lesion site. This suggests that the lesion site, and particularly the GFAP-negative area, remains a formidable barrier to regenerating axons from PTEN-deleted corticospinal neurons. Thus, a combination of PTEN deletion with other strategies such as neutralizing extracellular inhibitors at the lesion site[42,43] and bridging the lesion site with permissive grafts[44,45] may further promote maximal axon regeneration after spinal cord injury.

Taken together, our results indicate that immature neurons with high regenerative ability[46,47] have a high-level mTOR activity. mTOR activity undergoes a development-dependent down-regulation in many types of CNS neurons in addition to corticospinal neurons, suggesting that lack of mTOR activation is a general neuron-intrinsic mechanism underlying the diminished regenerative ability in the adult CNS. Together with optic nerve

regeneration observed after PTEN deletion[18], our results strongly support that re-activation of the mTOR pathway allows adult neurons to regain some of the growth capacities characteristic of young neurons. This “rejuvenation” strategy may be widely applicable for promoting successful regeneration following many types of injuries or traumas in the adult CNS.

METHODS

Animals and Surgeries

All experimental procedures were performed in compliance with animal protocols approved by the IACUC at Children’s Hospital, Boston. AAV preparation was described in Park et al[18].

For AAV injection, neonatal *PTEN*$^{f/f}$ were cryoanesthetized and injected with 2 μl of either AAV-Cre or AAV-GFP into the right sensorimotor cortex by using a nanolitter injector attached with a fine glass pipette. Mice were then placed on a warming pad and returned to the mothers after regaining normal colour and activity. For the mice at the age of 4 weeks, a total l.5 μl of AAV-Cre or AAV-GFP was injected into the hindlimb sensorimotor cortex at three sites (coordinates from bregma in mm: AP/ML/DV 0.0/1.5/0.5, −0.5/1.5/0.5, −1.0/1.5/0.5). The mice were placed on a warming blanket held at 37°C till fully awake and received a spinal cord lesion 4 weeks later.

For pyramidotomy, animals were anesthetized with ketamine/xylazine. The procedure is similar to what described previously[19,20]. Briefly, an incision was made at the left side of the trachea. Blunt dissection was performed to expose the skull base, and a craniotomy in the occipital bone allowed for access to the medullary pyramids. The left or right pyramid was cut with a fine scalpel medially up to the basilar artery. The wound was closed in layers with 6.0 sutures. The mice were placed on soft bedding on a warming blanket held at 37°C till fully awake. Two weeks later the intact CST was traced with BDA.

The procedure for T8 dorsal hemisection is similar to what was described previously[24–28]. Briefly, a midline incision was made over the thoracic vertebrae. A T8 laminectomy was performed. To produce a dorsal hemisection injury, the dorsal spinal cord was first cut with a pair of microscissors to the depth of 0.8 mm and then a fine microknife was drawn bilaterally across the dorsal aspect of the spinal cord. The muscle layers were sutured and the skin was secured with wound clips. The mice were placed on soft bedding on a warming blanket held at 37°C till fully awake. Urine was expressed by manual abdominal pressure twice daily till mice regained reflex bladder function. Six weeks post-injury, BDA was injected into the sensorimotor cortex to tract the CST.

The procedure of T8 spinal cord crush is similar to what was described previously[29,30] with modifications. Briefly, a midline incision was made over the thoracic vertebrae. A T8 laminectomy was performed. The exposed cord was crushed for 2 seconds with modified no. 5 jeweler’s forceps, keeping the dura intact. The muscle layers were sutured and the skin was secured with wound clips. The mice were placed on soft bedding on a warming blanket held at 37°C till fully awake. Urine was expressed by manual abdominal pressure twice

daily for the entire duration of the experiment. At 10 weeks post-injury the CST was traced with BDA.

BDA Tracing

To label CST axons by anterograde tracing, a total of l.6 μl of BDA (10%, Invitrogen) was injected into sensorimotor cortex at four sites (AP coordinates from bregma in mm: AP 1.0/1.5, 0.5/1.5, −0.5/1.5, −1.0/1.5 all at a depth of 0.5 mm into cortex). Mice were kept for an additional 2 weeks before termination.

Microruby retrograde labelling

This procedure is similar to what was described previously with modifications[48],[49]. Briefly, a C3 laminectomy was performed and 1 μl Microruby tracer (3000 MW, 5%, Invitrogen) was injected into the dorsal CST at the C3 spinal cord in 10 minutes. The pyramidotomy or sham surgery was performed 1 week later. Another week later, the intensities of p-S6 signals in microruby-labeled corticospinal neurons (CSMNs) were measured by using the Analyze Particle Tool in Image J software.

Preparation for histology and immunohistochemistry

Animals were given a lethal overdose of anaesthesia and transcardially perfused with 4% paraformaldehyde. Brains and spinal cords were isolated and post-fixed in the same fixative overnight at 4°C. Tissues were cryoprotected through increasing concentrations of sucrose. After embedding into OCT compound, the samples were snap-frozen in dry ice. Serial sections (25 μm) were collected and stored at −20°C until processed. Coronal sections of the sensorimotor cortex were cut for either p-S6 staining or PLAP staining. Coronal sections of the lower medulla were cut for counting BDA-labeled CST fibers. Transverse sections of intact spinal cords at identified levels (C4, C7 and T8) were collected to examine the projection pattern of CST axons. For mice with pyramidotomy, lesion sites at the medulla were carefully examined. Transverse sections of the cervical spinal cord were stained with PKCγ antibody (Santa Cruz Biotechnology, sc-211, 1:100) to further examine the completeness of the lesion (data not shown). Mice with incomplete lesion were excluded from the study. For assessing the extent of CST sprouting, serial sections of C7 spinal cords were cut in the transverse plane. For mice with T8 lesion, serial sections of the spinal cord region containing the lesion site were cut in the sagittal plane. Transverse sections of the caudal cord (5 mm and 3 mm to the lesion respectively) were taken to exclude incomplete lesions.

Immunofluorescence staining of the spinal cord, cortex and medulla

Immunostaining was performed following standard protocols. All antibodies were diluted in a solution consisting of 10% normal goat serum (NGS) and 1% Triton X-100 in phosphate-buffered saline (PBS). Antibodies used were rabbit anti-p-S6 (Ser235/236) (1:200, Cell Signalling Technology) and rabbit anti-GFAP (1:1,000, DAKO). Sections were incubated with primary antibodies overnight at 4°C and washed three times for 10 minutes with PBS. Secondary antibodies (goat-anti-rabbit Alexa488) were then applied and incubated for 1 hour at room temperature. To detect BDA labeled fibers, BDA staining was performed by

incubating the sections in PBS containing streptavidin-HRP. The remaining staining procedure was performed according to the protocol provided by TSA™ Cyanine 3 system (Perkin Elmer).

Preparation for electron microscopy

Two mice with T8 crush injuries received unilateral injections of BDA into the sensorimotor cortex at 10 weeks post-injury and were perfused with 4% paraformaldehyde 2 weeks later. An approximately 8mm segment of the spinal cord containing the lesion site was sectioned in the sagittal plane on a Vibratome® at 50μm. Sections were incubated for 1 h with avidin and biotinylated HRP (Vectastain ABC kit; Vector Laboratories), washed in PBS, and then reacted with DAB in 50mM Tris buffer, pH 7.6, 0.024% hydrogen peroxide, and 0.5% nickel chloride. The sections were examined under a light microscope while still wet. Serial sections with BDA labeled axons caudal to the injury were selected for electron microscopic analysis.

The selected sections were rinsed in 0.1 M cacodylate buffer and postfixed with 1 % osmium tetroxide in 0.1 M cacodylate buffer for 1 hour, rinsed in ddH20 for 2 × 10 min., dehydrated in increasing serial dilutions of ethanol (70%, 85%, 95%, 100% × 2) for 10 min each, put in propylene oxide (intermediate solvent) for 2 × 10 min, incubated in propylene oxide/Spurr's resin (1:1 mix) for 30 min, and in Spurr's resin overnight. Sections were flat-embedded between two sheets of "Aclar" film and polymerized overnight at 60° Celsius.

Images were taken of each section and imported into Adobe Photoshop. Tracings were made of the BDA labeled axons present in each image. Then the tracings were aligned and collapsed into a single image so as to reveal the BDA labeled axons in the collection of sections. One section of the series was chosen for electron microscopic analysis, and a collection of bouton-like swellings on the regenerated axons were identified in advance. Ultrathin sections of 60 nm thickness were cut, mounted on copper grids and viewed using a JEOL 1400 electron microscope. Individual BDA-labeled boutons were then located and assessed at the electron microscopic level.

Axonal counting and quantifications

For quantifying total labeled CST axon, BDA labeled CST fibers were counted at the level of medulla oblongata 1 mm proximal to the pyramidal decussation. Axons were counted in 4 rectangular areas (9506 μm^2) per section on two adjacent sections. The number of labeled axons was calculated by multiplying with the total area.

For the groups of pyramidotomy, digital images of C7 spinal cord transverse sections were collected by using a Nikon fluorescence microscope under a 4× objective. Densitometry measurement on each side of the gray matter was taken by using Metamorph software, after being sub-thresholded to the background and normalized by area. The outcome measure of the sprouting density index was the ratio of contralateral and ipsilateral counts. At least 3 sections were measured for each mouse.

To quantify the number of sprouting axons, a horizontal line was firstly drawn through the central canal and across the lateral rim of the gray matter. Three vertical lines (Mid, Z1, and

Z2) were then drawn to divide the horizontal line into three equal parts, starting from the central canal to the lateral rim. While Mid denotes midline crossing fibers, Z1 and Z2 are for sprouting fibers at different distance from the midline. Only fibers crossing the three lines were counted on each section. The results were presented after normalization with the number of counted CST fibers at the medulla level. At least 3 sections were counted for each mouse.

In the animals of T8 dorsal hemisection, digital images were taken at the CST end by using a confocal microscope (Zeiss, LSM510) under a 63× objective to quantify the number of retraction bulbs,. The number of bulbs was counted within a square by the area of 21389 μm^2 and normalized by the number of BDA labeled CST at the medulla. At least 3 sections with the main CST per animal were examined. The results were presented as the number of retraction bulbs per 0.1 mm^2 per labeled CST.

The density of sprouting fibers of the main CST rostral to the lesion site was analyzed quantitatively using digital images taken with a Nikon fluorescence microscope under a 4× objective. A series of rectangular segments by the width of 100 μm and the height covering the dorsal-ventral aspect of the cord were superimposed onto the sagittal sections, starting from 1.5 mm rostral up to the lesion center. After subtracting the background (the most caudal part of the section), the pixel value of each segment was normalized by dividing with the first segment (1.5 mm rostral). The results were presented as a ratio at different distances (fiber density index). Every other section of the whole spinal cord was stained. 3–4 sections with main CST per animal were quantified.

The number of fibers caudal to the lesion was analyzed with a fluorescence microscope. The number of intersections of BDA-labeled fibers with a dorsal-ventral line positioned at a defined distance caudal from the lesion center was counted under a 40× objective. Every other section of the whole spinal cord was stained. Fibers were counted on 3–4 sections with the main dorsal CST and 1–3 lateral sections with collaterals in the gray matter. The number of counted fibers was normalized by the number of labeled CST axons in the medulla and divided by the number of evaluated sections. This resulted in the number of CST fibers per labeled CST axons per section at different distances (fiber number index).

For the animals with T8 crush, the number of fibers caudal to the lesion was analyzed with a fluorescence microscope. The number of intersections of BDA-labeled fibers with a dorsal-ventral line positioned at a defined distance caudal from the lesion center was counted under a 40× objective. Every other section of the whole spinal cord was stained. Fibers were counted on 3 sections with the main dorsal CST. The number of counted fibers was normalized by the number of labeled CST axons in the medulla and divided by the number of evaluated sections. This resulted in the number of CST fibers per labeled CST axon per section at different distances (fiber number index).

Statistical analysis

Two-tailed Student’s t-test was used for the single comparison between two groups. The rest of the data were analyzed using one-way or two-way ANOVA depending on the appropriate design. *Post hoc* comparisons were carried out only when a main effect showed statistical

significance. P-value of multiple comparisons was adjusted by using Bonferroni's correction. All analyses were conducted through StatView. Data are presented as means ± SEM and the asterisks indicate statistical significance under an appropriate test.

Supplementary Material

Refer to Web version on PubMed Central for supplementary material.

Acknowledgments

We thank Dr. F. Wang for providing Rosa-stop-PLAP mice and Drs. M. Greenberg. M. Tessier-Lavigne, and C. Woolf for reading the manuscript. Supported by grants from Wings for Life (KL), Craig H. Neilson Foundation (YL and KP), NINDS, Wings for Life, and International Spinal Research Trust (ZH), NINDS (BZ), NINDS and private contribution to the Reeve-Irvine Reserch Center (OS). RW is the recipient of a predoctoral fellowship from NINDS.

References

1. Raineteau O, Schwab ME. Plasticity of motor systems after incomplete spinal cord injury. Nat Rev Neurosci. 2001; 2:263–273. [PubMed: 11283749]
2. Blesch A, Tuszynski MH. Spinal cord injury: plasticity, regeneration and the challenge of translational drug development. Trends Neurosci. 2009; 32:41–47. [PubMed: 18977039]
3. Zheng B, Lee JK, Xie F. Genetic mouse models for studying inhibitors of spinal axon regeneration. Trends Neurosci. 2006; 29:640–646. [PubMed: 17030430]
4. Deumens R, Koopmans GC, Joosten EA. Regeneration of descending axon tracts after spinal cord injury. Prog Neurobiol. 2005; 77:57–89. [PubMed: 16271433]
5. Thallmair M, Metz GA, Z'Graggen WJ, Raineteau O, Kartje GL, Schwab ME. Neurite growth inhibitors restrict plasticity and functional recovery following corticospinal tract lesions. Nat Neurosci. 1998; 1:124–31. [PubMed: 10195127]
6. Cafferty WB, Strittmatter SM. The Nogo-Nogo receptor pathway limits a spectrum of adult CNS axonal growth. J Neurosci. 2006; 26:12242–50. [PubMed: 17122049]
7. Case LC, Tessier-Lavigne M. Regeneration of the adult central nervous system. Curr Biol. 2005; 15:R749–53. [PubMed: 16169471]
8. Schnell L, Schwab ME. Axonal regeneration in the rat spinal cord produced by an antibody against myelin-associated neurite growth inhibitors. Nature. 1990; 343:269–272. [PubMed: 2300171]
9. Savio T, Schwab ME. Lesioned corticospinal tract axons regenerate in myelin-free rat spinal cord. Proc Natl Acad Sci U S A. 1990; 87:4130–4133. [PubMed: 2349222]
10. García-Alías G, Barkhuysen S, Buckle M, Fawcett JW. Chondroitinase ABC treatment opens a window of opportunity for task-specific rehabilitation. Nat Neurosci. 2009; 12:1145–1151. [PubMed: 19668200]
11. Leaver SG, et al. AAV-mediated expression of CNTF promotes long-term survival and regeneration of adult rat retinal ganglion cells. Gene Ther. 2006; 13:1328–1341. [PubMed: 16708079]
12. Schnell L, Schneider R, Kolbeck R, Barde YA, Schwab ME. Neurotrophin-3 enhances sprouting of corticospinal tract during development and after adult spinal cord lesion. Nature. 1994; 367:170–173. [PubMed: 8114912]
13. Hiebert GW, Khodarahmi K, McGraw J, Steeves JD, Tetzlaff W. Brain-derived neurotrophic factor applied to the motor cortex promotes sprouting of corticospinal fibers but not regeneration into a peripheral nerve transplant. J Neurosci Res. 2002; 69:160–168. [PubMed: 12111797]
14. Hollis ER 2nd, Lu P, Blesch A, Tuszynski MH. IGF-I gene delivery promotes corticospinal neuronal survival but not regeneration after adult CNS injury. Exp Neurol. 2009; 215:53–59. [PubMed: 18938163]

15. David S, Aguayo AJ. Axonal elongation into peripheral nervous system “bridges” after central nervous system injury in adult rats. Science. 1981; 214:931–933. [PubMed: 6171034]
16. Richardson PM, Issa VM, Aguayo AJ. Regeneration of long spinal axons in the rat. J Neurocytol. 1984; 13:165–82. [PubMed: 6707710]
17. Bregman BS, Kunkel-Bagden E, McAtee M, O’Neill A. Extension of the critical period for developmental plasticity of the corticospinal pathway. J Comp Neurol. 1989; 282:355–370. [PubMed: 2715387]
18. Park KK, et al. Promoting axon regeneration in the adult CNS by modulation of the PTEN/mTOR pathway. Science. 2008; 322:963–966. [PubMed: 18988856]
19. Bareyre FM, et al. The injured spinal cord spontaneously forms a new intraspinal circuit in adult rats. Nat Neurosci. 2004; 7:269–277. [PubMed: 14966523]
20. Weidner N, Ner A, Salimi N, Tuszynski MH. Spontaneous corticospinal axonal plasticity and functional recovery after adult central nervous system injury. Proc Natl Acad Sci U S A. 2001; 98:3513–3518. [PubMed: 11248109]
21. Ma XM, Blenis J. Molecular mechanisms of mTOR-mediated translational control. Nat Rev Mol Cell Biol. 2009; 10:307–318. [PubMed: 19339977]
22. Groszer M, et al. Negative regulation of neural stem/progenitor cell proliferation by the Pten tumor suppressor gene in vivo. Science. 2001; 294:2186–2189. [PubMed: 11691952]
23. Hasegawa H, Wang F. Visualizing mechanosensory endings of TrkC-expressing neurons in HS3ST-2-hPLAP mice. J Comp Neurol. 2008; 511:543–556. [PubMed: 18839409]
24. Bareyre FM, Kerschensteiner M, Misgeld T, Sanes JR. Transgenic labeling of the corticospinal tract for monitoring axonal responses to spinal cord injury. Nat Med. 2005; 11:1355–1360. [PubMed: 16286922]
25. Simonen M, et al. Systemic deletion of the myelin-associated outgrowth inhibitor Nogo-A improves regenerative and plastic responses after spinal cord injury. Neuron. 2003; 38:201–211. [PubMed: 12718855]
26. Kim JE, Li S, GrandPre T, Qiu D, Strittmatter SM. Axon regeneration in young adult mice lacking Nogo-A/B. Neuron. 2003; 38:187–199. [PubMed: 12718854]
27. Zheng B, et al. Lack of enhanced spinal regeneration in Nogo-deficient mice. Neuron. 2003; 38:213–224. [PubMed: 12718856]
28. Steward O, et al. Regenerative growth of corticospinal tract axons via the ventral column after spinal cord injury in mice. J Neurosci. 2008; 28:6836–6847. [PubMed: 18596159]
29. Fujiki M, Zhang Z, Guth L, Steward O. Genetic influences on cellular reactions to spinal cord injury: activation of macrophages/microglia and astrocytes is delayed in mice carrying a mutation (WldS) that causes delayed Wallerian degeneration. J Comp Neurol. 1996; 371:469–484. [PubMed: 8842900]
30. Inman DM, Steward O. Ascending sensory, but not other long-tract axons, regenerate into the connective tissue matrix that forms at the site of a spinal cord injury in mice. J Comp Neurol. 2003; 462:431–449. [PubMed: 12811811]
31. Tom VJ, Steinmetz MP, Miller JH, Doller CM, Silver J. Studies on the development and behavior of the dystrophic growth cone, the hallmark of regeneration failure, in an in vitro model of the glial scar and after spinal cord injury. J Neurosci. 2004; 24:6531–6539. [PubMed: 15269264]
32. Lee JK, Chan AF, Luu SM, Zhu Y, Ho C, Tessier-Lavigne M, Zheng B. Reassessment of corticospinal tract regeneration in Nogo-deficient mice. J Neurosci. 2009; 29:8649–8654. [PubMed: 19587271]
33. Bundesen LQ, Scheel TA, Bregman BS, Kromer LF. Ephrin-B2 and EphB2 regulation of astrocyte-meningeal fibroblast interactions in response to spinal cord lesions in adult rats. J Neurosci. 2003; 23:7789–7800. [PubMed: 12944508]
34. Maier IC, Baumann K, Thallmair M, Weinmann O, Scholl J, Schwab ME. Constraint-induced movement therapy in the adult rat after unilateral corticospinal tract injury. J Neurosci. 2008; 28:9386–9403. [PubMed: 18799672]
35. Varoqui H, Schäfer MK, Zhu H, Weihe E, Erickson JD. Identification of the differentiation-associated Na+/PI transporter as a novel vesicular glutamate transporter expressed in a distinct set of glutamatergic synapses. J Neurosci. 2002; 22:142–155. [PubMed: 11756497]

36. Persson S, Boulland JL, Aspling M, Larsson M, Fremeau RT Jr, Edwards RH, Storm-Mathisen J, Chaudhry FA, Broman J. Distribution of vesicular glutamate transporters 1 and 2 in the rat spinal cord, with a note on the spinocervical tract. J Comp Neurol. 2006; 497:683–701. [PubMed: 16786558]
37. Zhou FQ, Zhou J, Dedhar S, Wu YH, Snider WD. NGF-induced axon growth is mediated by localized inactivation of GSK-3beta and functions of the microtubule plus end binding protein APC. Neuron. 2004; 42:897–912. [PubMed: 15207235]
38. Park KK, Liu K, Hu Y, Kanter JL, He Z. PTEN/mTOR and axon regeneration. Exp Neurol. 2010; 223:45–50. [PubMed: 20079353]
39. Zhao M, Song B, Pu J, Wada T, Reid B, Tai G, Wang F, Guo A, Walczysko P, Gu Y, Sasaki T, Suzuki A, Forrester JV, Bourne HR, Devreotes PN, McCaig CD, Penninger JM. Electrical signals control wound healing through phosphatidylinositol-3-OH kinase-gamma and PTEN. Nature. 2006; 442:457–460. [PubMed: 16871217]
40. Yin HS, Selzer ME. Axonal regeneration in lamprey spinal cord. J Neurosci. 1983; 3:1135–1144. [PubMed: 6854366]
41. Bernstein JJ, Gelderd JB. Synaptic reorganization following regeneration of goldfish spinal cord. Exp Neurol. 1973; 41:402–410. [PubMed: 4746201]
42. Garcia-Alias G, Barkhuysen S, Buckle M, Fawcett JW. Chondroitinase ABC treatment opens a window of opportunity for task-specific rehabilitation. Nat Neurosci. 2009; 12:1145–1151. [PubMed: 19668200]
43. Houle JD, Tom VJ, Mayes D, Wagoner G, Phillips N, Silver J. Combining an autologous peripheral nervous system “bridge” and matrix modification by chondroitinase allows robust, functional regeneration beyond a hemisection lesion of the adult rat spinal cord. J Neurosci. 2006; 26:7405–7415. [PubMed: 16837588]
44. Alto LT, Havton LA, Conner JM, Hollis Ii ER, Blesch A, Tuszynski MH. Chemotropic guidance facilitates axonal regeneration and synapse formation after spinal cord injury. Nat Neurosci. 2009; 12:1106–1113. [PubMed: 19648914]
45. Pearse DD, Pereira FC, Marcillo AE, Bates ML, Berrocal YA, Filbin MT, Bunge MB. cAMP and Schwann cells promote axonal growth and functional recovery after spinal cord injury. Nat Med. 2004; 10:610–616. [PubMed: 15156204]
46. Kennard MA. age and other factors in motor recovery from precentral lesions in monkeys. Am J Physiol. 1936; 115:138–146.
47. Berger W. Characteristics of locomotor control in children with cerebral palsy. Neurosci Biobehav Rev. 1998; 22:579–582. [PubMed: 9595572]
48. Courtine G, Song B, Roy RR, Zhong H, Herrmann JE, Ao Y, Qi J, Edgerton VR, Sofroniew MV. Recovery of supraspinal control of stepping via indirect propriospinal relay connections after spinal cord injury. Nat Med. 2008; 14:69–74. [PubMed: 18157143]
49. Arlotta P, Molyneaux BJ, Chen J, Inoue J, Kominami R, Macklis JD. Neuronal subtype-specific genes that control corticospinal motor neuron development in vivo. Neuron. 2005; 45:207–221. [PubMed: 15664173]

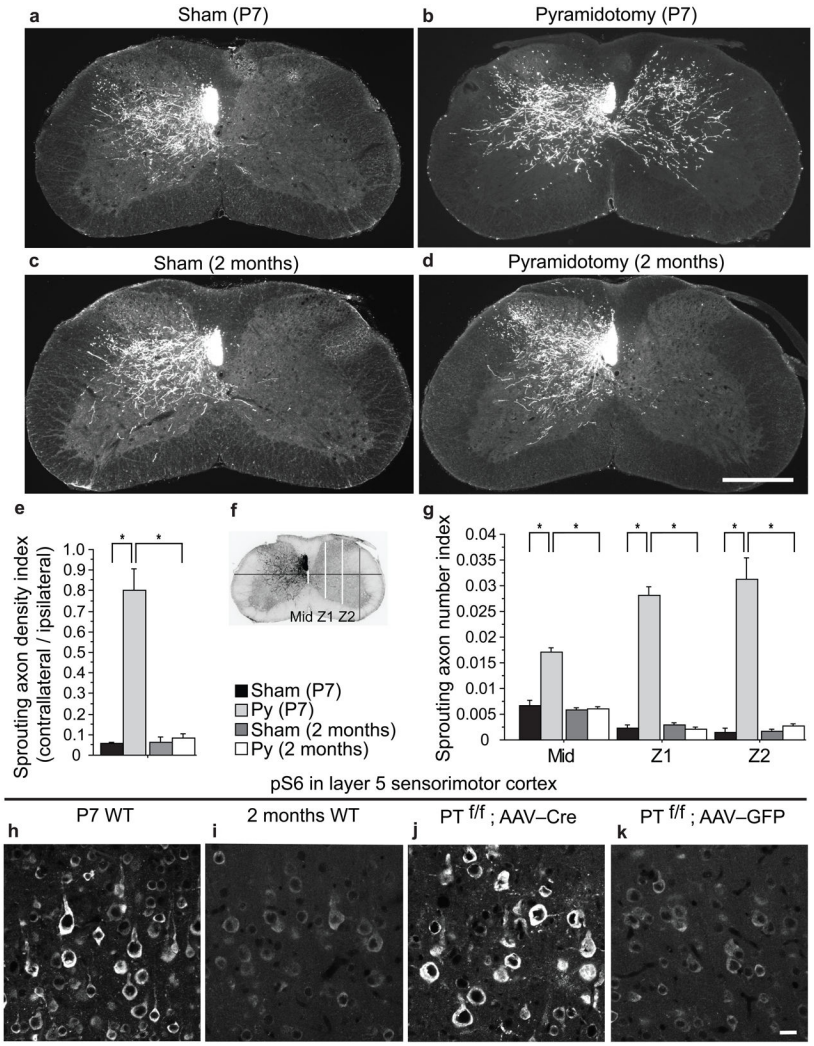

Figure 1. Correlation between age-dependent decrease of CST sprouting and phospho-S6 levels in corticospinal neurons

a–d, Representative images of cervical 7 (C7) spinal cord transverse sections from wild-type mice with a left pyramidotomy (Py) performed at P7 (**b**) or 2 months (**d**) and their respective controls (**a**, **c**). BDA was injected to the right sensorimotor cortex at 2 weeks post-injury and mice were terminated 2 weeks later. Scale bar: 500 μm. **e**, Quantification of sprouting axon density index (contralateral/ispilateral). *: $p < 0.01$, ANOVA followed by Bonferroni's post-hoc test. **f**, Scheme of quantifying crossing axons at different regions of the spinal cord (Mid: midline, Z1 or Z2: different lateral positions). **g**, Quantification results with the methods indicated in (**f**) and then normalized against total numbers of labeled CST axons counted at the medulla in each animal. *: $p < 0.01$, two-way ANOVA followed by Bonferroni's post-hoc test. For the quantification results in **e–g**, 4 mice in each of the control groups and 5 mice in the P7 groups and 7 mice in the 2 months groups were used. Three sections at the C7 level per animals were quantified. **f–k**, Representative images of the coronal sections of the layer 5 sensorimotor cortex from wild type mice at P7 (**h**) or 2

months (**i**) or 2 months-old *PTEN*$^{f/f}$ (*PT*$^{f/f}$) mice of with AAV-Cre (**j**) or AAV-GFP (**k**). Scale bar: 20 μm.

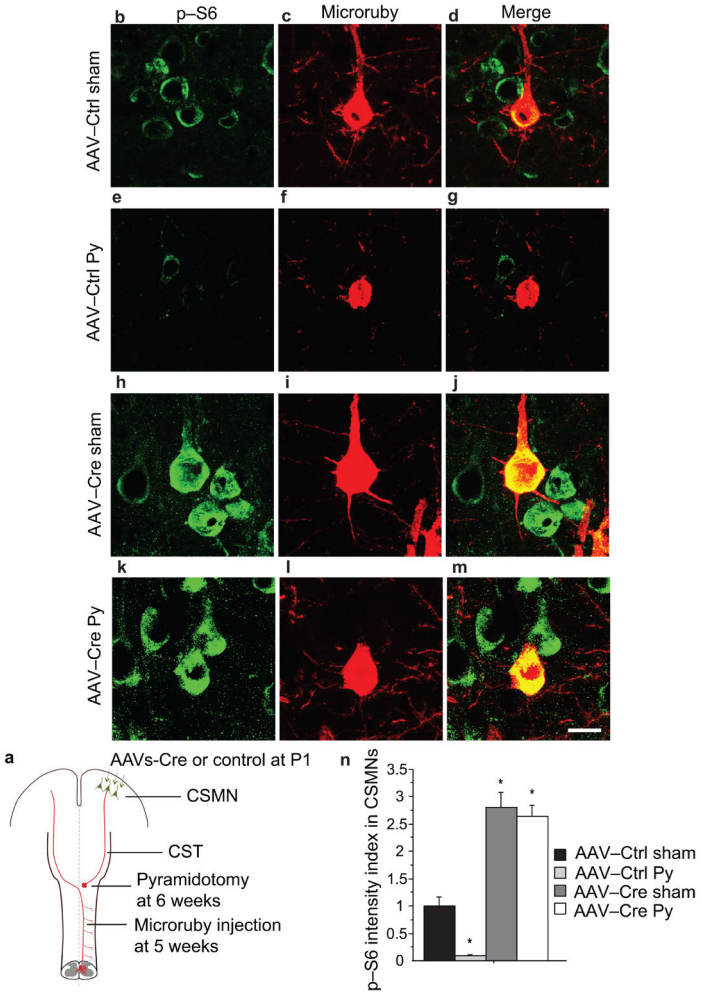

Figure 2. *PTEN* deletion prevents p-S6 down-regulation in corticospinal neurons after pyramidotomy

a, The experimental scheme to assess the p-S6 levels in the corticospinal neurons (CSMNs) in the sensorimotor cortex for the experiments shown in **b–n**. AAVs were injected to right cortex at P1 and the animals were subjected to C7 microruby injection at the age of 5 weeks and right pyramidotomy at the age of 6 weeks. The animals were terminated at 7 days after injury for p-S6 detection. **b–m,** Representative images of sagittal sections from the sham (**b–d, h–j**) or injured (**e–g, k–m**) side of layer 5 sensorimotor cortex from *PTEN*$^{f/f}$ mice injected with control AAV (**b–g**) or AAV-Cre (**h–m**) stained with anti-p-S6 (**b, e, h, k**) or retrogradely labeled with microruby (**c, f, i, l**). The panels in (**d, g, j, m**) are the merged images. Scale bar: 20 μm. **n**, The quantification results of average p-S6+ intensity of CSMNs in comparison with that in intact ones. The intensities of more than 300 CSMNs from 3 animals in each group were quantified. $p < 0.001$, ANOVA followed by Bonferroni's post-hoc test.

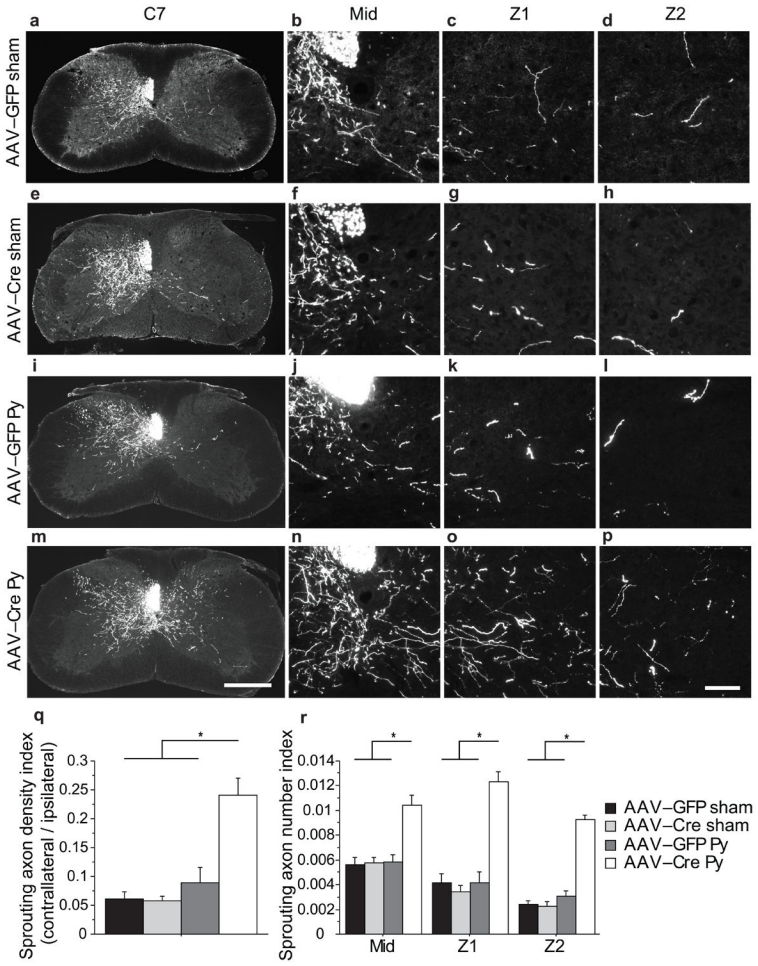

Figure 3. *PTEN* deletion promotes CST sprouting in adult mice with unilateral pyramidotomy

a–p, Representative images of C7 spinal cord transverse sections (**a**, **e**, **i**, **m**), enlarged midline (**b**, **f**, **j**, **n**), Z1 (**c**, **g**, **k**, **o**), or Z2 (**d**, **h**, **l**, **p**) regions from sham (**a–h**) or injured (**i–p**) *PTEN*$^{f/f}$ mice with AAV-GFP (**a–d**, **i–l**) or AAV-Cre (**e–h**, **m–p**). AAVs were injected to the right sensorimotor cortex of P1 *PTEN*$^{f/f}$ mice that then received a left pyramidotomy or sham lesion at 2 months. BDA was injected to the right sensorimotor cortex at 2 weeks post-injury and the animals were terminated 2 weeks later. **q**, Quantification of sprouting axon density index (contralateral/ispilateral). *: $p < 0.01$, ANOVA followed by Bonferroni's post-hoc test. **r**, Quantifications of crossing axons counted in different regions of spinal cord normalized against the numbers of labeled CST axons. *: $p < 0.01$, two-way ANOVA followed by Bonferroni's post-hoc test. Five animals in each intact group and 6 animals in each pyramidotomy group were used. Three C7 spinal cord sections per animals were quantified. Scale bar: 500 μm (**a**, **e**, **i**, **m**), 50 μm (**b–d**, **f–h**, **j–l**, and **n–p**).

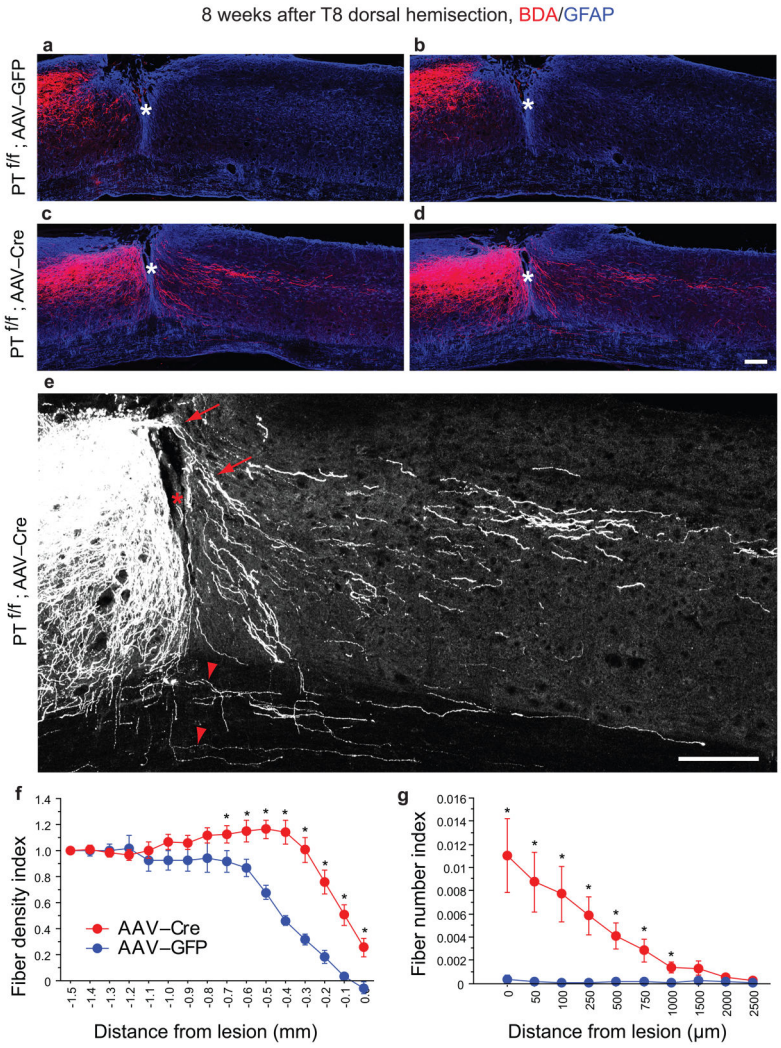

Figure 4. Increased CST regrowth in *PTEN* deleted mice after T8 dorsal hemisection

a–d, Representative images from sagittal sections from *PTEN*$^{f/f}$ mice with right cortical injection of AAV-GFP (**a**, **b**) or AAV-Cre (**c**, **d**) at P1 and T8 dorsal hemisection at 6 weeks. BDA was injected to the right sensorimotor cortex at 6 weeks post-injury and the animals were terminated 2 weeks later. The sections were co-stained to detect BDA (red) and GFAP (blue). **e**, Enlarged images in (**d**) showing two types of labeled axons growing to the distal spinal cord: growing through the lesion sites (red arrow) and sprouting through the intact ventral spinal cord (red arrowhead). Red star denotes the lesion site. **f**, Quantification of the density of labeled CST axons in the spinal cord rostral to the lesion sites in two groups. *: $p < 0.05$, two–way ANOVA followed by Fisher's LSD. **g**, Quantification of the CST axons quantified in the spinal cord distal to the lesion sites. *: $p < 0.05$, two-way ANOVA followed by Fisher's LSD. 9 animals in AAV-GFP group and 11 in AAV-Cre groups were used. 4–5 sections per animals were quantified. Scale bar: 200 μm.

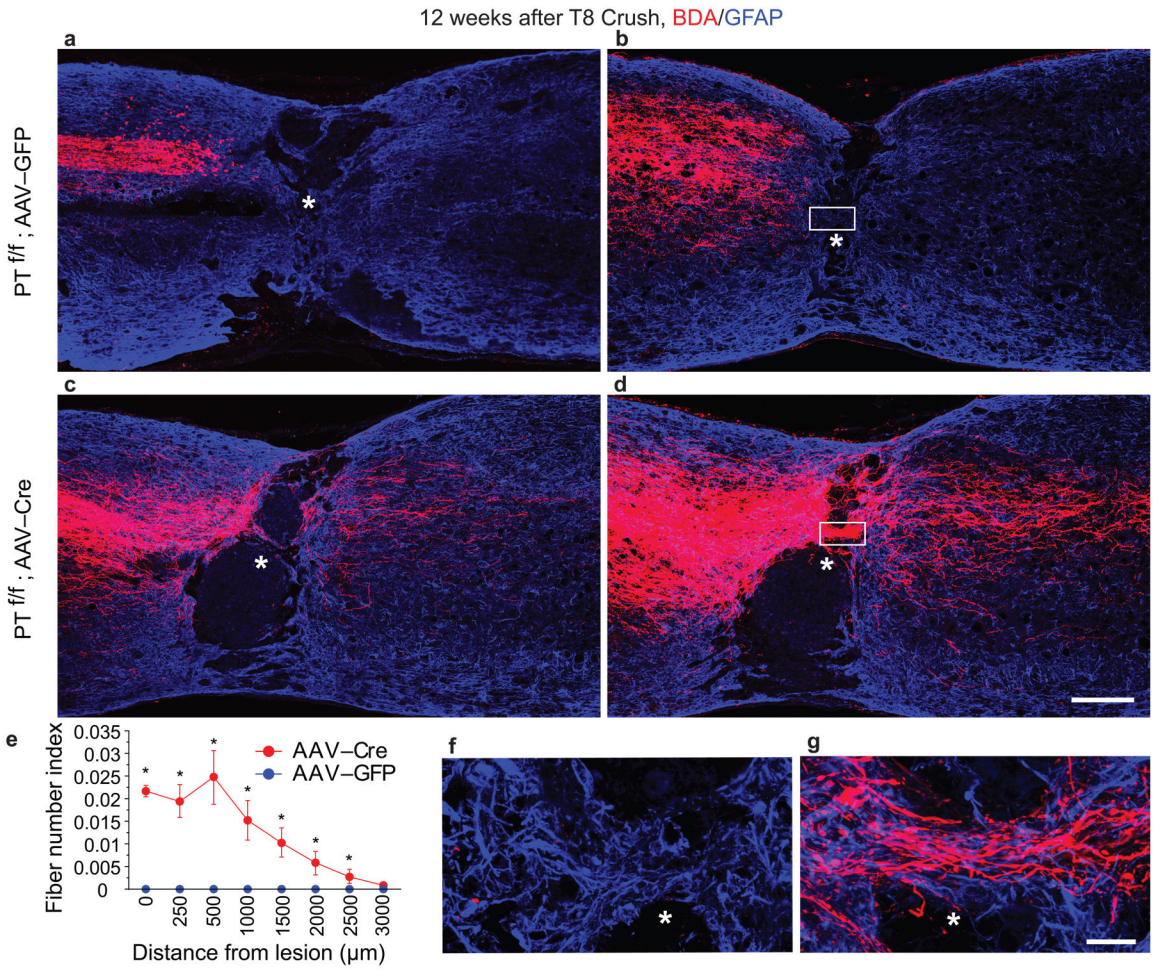

Figure 5. CST regeneration in *PTEN* deleted mice after a T8 spinal cord crush injury

a–d, Representative images from sagittal sections showing the main dorsal CST tract (**a**, **c**) or lateral CST axons in the gray matter (**b**, **d**) in *PTEN*$^{f/f}$ mice with cortical injection of AAV-GFP (**a**, **b**) or AAV-Cre (**c**, **d**) at P1 and T8 crush injury at 6 weeks. BDA was injected to the sensorimotor cortex at 10 weeks after injury and the animals were terminated 2 weeks later. The sections were co-stained to detect BDA (red) and GFAP (blue). In contrast to control mice in which no labeled axons can be seen within or beyond the lesion, numerous axons grow through the lesion site and are detected in the distal spinal cord (up to 3 mm). Scale bar: 200 μm. **e**, Quantification of labeled axons in the spinal cord caudal to the lesion site in both groups. *: $p < 0.05$, two-way ANOVA followed by Fisher's LSD. Eight animals in each group were used. Three sections per animals were quantified. **f**, **g**, Immunoflurorescent images showing sections from the matrix of the lesion sites of crushed PTEN$^{f/f}$ mice with AAV-GFP (**f**) or AAV-Cre (**g**) detected with TSA-Cy3 (for BDA) and anti-GFAP antibodies. Scale bar: 20 μm.

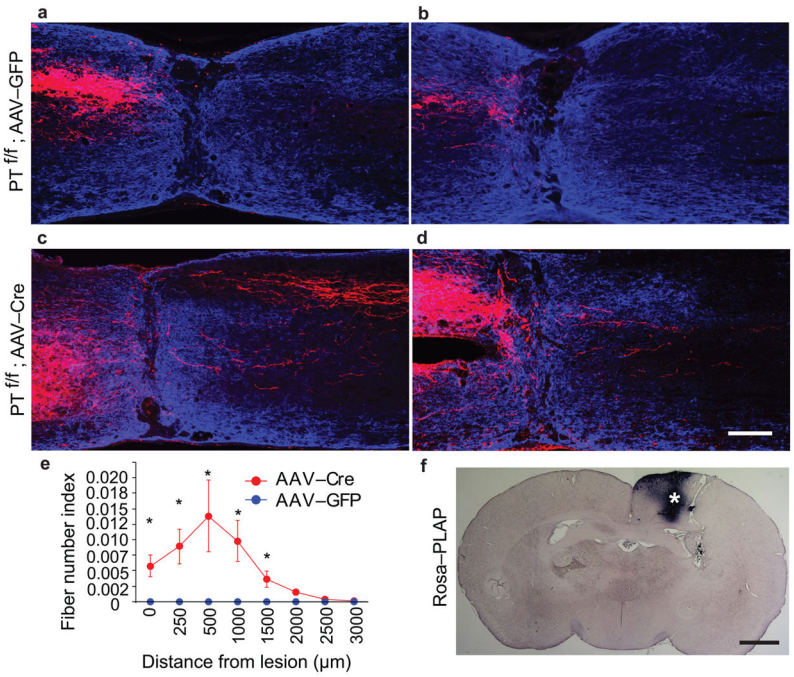

Figure 6. CST regeneration in *PTEN*$^{f/f}$ mice with AAV injection at 4 weeks and T8 spinal cord crush injury at 8 weeks

a–d, Representative images from sagittal sections showing the main dorsal CST tract (**a**, **c**) or lateral CST axons in the gray matter (b, d) in *PTEN*$^{f/f}$ mice with cortical injection of AAV-GFP (**a**, **b**) or AAV-Cre (**c**, **d**) at the age of 4 weeks and T8 crush injury at 8 weeks. BDA was injected to the sensorimotor cortex at 10 weeks after injury and the animals were terminated 2 weeks later. The sections were co-stained to detect BDA (red) and GFAP (blue). Scale bar: 200 μm. **e**, Quantification of labeled axons in the spinal cord caudal to the lesion site in both groups. *: $p < 0.05$, two-way ANOVA followed by Fisher's LSD. 5 animals in each group were used. 3 sections per animals were quantified. **f**, PLAP staining of a cortical section from a reporter mouse with AAV-Cre injection at the age of 4 weeks. By examining different sections covering entire hindlimb sensorimotor cortex, estimated PLAP+ areas in these mice is about 20% of the area of the reporter mice with neonatal AAV-Cre injection. Scale bar: 1 mm.

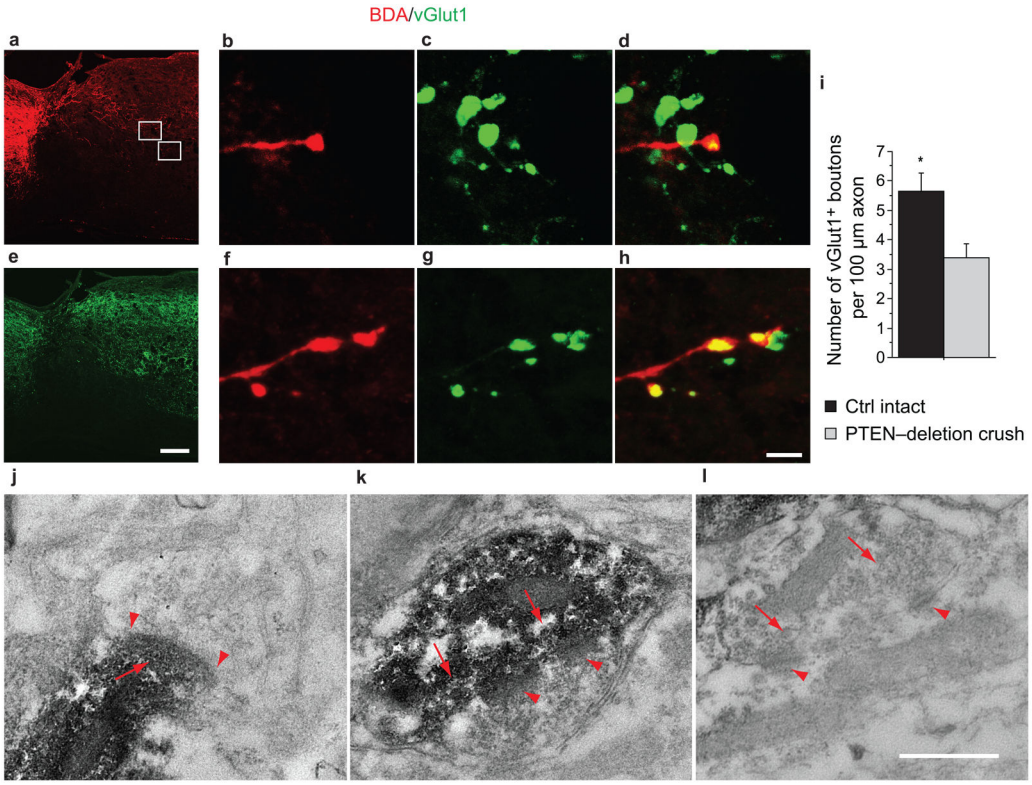

Figure 7. Regenerating CST axons after *PTEN* deletion form synapse-structures in spinal segments caudal to a crush injury

a,b, Sagittal sections from *PTEN*$^{f/f}$ mice with AAV-Cre injection at P1, T8 spinal cord crush at the age of 6 weeks, BDA tracing at the age of 16 weeks and terminated at the age 18 weeks were analyzed for BDA (**a**) and vGlut1 (**b**) signals. Note that anti-vGlut1 antibodies label synaptic boutons of both CST axons and sensory axons, consistent with previous reports[34–36]. The asterisk marks the crush site. Scale bar: 200 µm. **c–h**, Representative examples of BDA-labeled boutons (**c**, **f**) co-localizing with anti-vGlut1 signals (**d**, **g**) and their merged images (**e**, **h**) from the gray matter of the spinal cord caudal to the crush site (squares in **a**). Scale bar: 5 µm. **i,** Frequencies of vGlut1$^+$ boutons in BDA-labeled axons quantified mostly from the intermediate zone of the thoracic spinal cord gray matter in both intact control and *PTEN*$^{f/f}$ with AAV-Cre mice. Both the BDA-labeled axonal lengths and the BDA$^+$vGlut1$^+$ boutons from 15 sections of 3 mice in each group were quantified. In crushed PTEN-deletion mice, we found BDA/vGlut1 co-labeled synapse approximately 60% as frequently as in intact control mice. Student's t-test, $P<0.05$. Scale bar: 200µm (**a, b**) and bottom 5µm (**c–h**). **j–l**, Representative electron microscope images showing two synaptic structures formed by BDA-labeled axons (**j, k**) and a nearby unlabeled control synapse (**l**). In spinal neurons, the synaptic contact region often has patches of psd, which is the case in the synapse in **k**. In **j**, the psd is continuous between the arrows. sv: synaptic vesicle; psd: postsynaptic density.